Luminescent multi-terpyridine ligands: towards 2D polymer formation in solution

Journal:	*Photochemical & Photobiological Sciences*
Manuscript ID:	PP-ART-02-2014-000056.R2
Article Type:	Paper
Date Submitted by the Author:	23-Apr-2014
Complete List of Authors:	Gallina, Maria; Università di Bologna, Dipartimento di Chimica G. Ciamician Bergamini, Giacomo; Universita di Bologna, Dipartimento di Chimica G. Ciamician Di Motta, Simone; University of Bologna, Dipartimento di Chimica G. Ciamician Sakamoto, Junji; ETH, Department of Materials Negri, Fabrizia; Università di Bologna, of Chemistry 'Ciamician' Ceroni, Paola; Universita di Bologna, Dipartimento di Chimica G. Ciamician

Photochemical & Photobiological Sciences

Cite this: DOI: 10.1039/c0xx00000x

www.rsc.org/xxxxxx

ARTICLE TYPE

Luminescent multi-terpyridine ligands: towards 2D polymer formation in solution

Maria Elena Gallina,[a] Giacomo Bergamini,[a] Simone Di Motta,[a] Junji Sakamoto,[b] Fabrizia Negri,[a]* Paola Ceroni[a]*

Received (in XXX, XXX) Xth XXXXXXXXX 20XX, Accepted Xth XXXXXXXXX 20XX
DOI: 10.1039/b000000x

The investigated multiterpyridine chromophores form a 2D network upon metal ion complexation that causes profound changes to their photophysical properties; the experimental results are complemented by modeling of the electronic properties of isolated monomers as well as the structure of the polymeric network.

Introduction

2,2':6',2''-Terpyridine (tpy) is one of the most investigated ligand for d-block metal ions since it yields highly stable complexes with interesting optical, electronic and magnetic properties.[1,2] Its rich coordination chemistry has been widely employed to build up dyads and linear polynuclear metal complexes,[3] grids and racks,[4] metallomacrocycles,[5] as well as metal coordination polymers.[2a,6,7] The resulting metal complexes have potential applications in a variety of fields[2] ranging from light-to-electricity conversion and organic light-emitting diodes, to luminescent or electrochemical sensors and catalysts in (asymmetric) organic transformations.

Pristine terpyridine is weakly luminescent (Φ_{em} = 0.3%)[8] and has been decorated with a variety of fluorophores in order to combine luminescence and metal binding properties.[1,2] Another approach to get luminescent terpyridine molecules is extending the conjugation and the rigidity of the system by appending proper substituents in the 4' position.[2a] Although the phenyl and terpyridyl rings are not coplanar, the 4'-*p*-tolyl-2,2':6',2''-terpyridine (hereafter called **tol-tpy**) displays improved luminescent properties in the UV spectral region with 8% emission quantum yield in CH_2Cl_2 solution.[7b]

In the present work, the **tol-tpy** unit has been appended to a benzene core leading to highly luminescent multiterpyridine ligands (Φ_{em} ca. 35%), containing 3 and 6 binding sites, **M3** and **M6** respectively in Scheme 1. **M6** has been previously reported[9,10] to form, at the air/water interface, a free-standing monolayer sheet held together by metal ions: the tpy units of one **M6** molecule are bound to a tpy unit belonging to one of the six neighboring monomers by concomitant complexation of a metal ion (Scheme 2). In the present paper, we have investigated **M3** and **M6** as ligands of Zn^{2+} and Fe^{2+} ions in dichloromethane solution. At low metal ion concentration, complexes of 2:1 tpy to metal ion ratio are formed in both cases, giving rise to a polymeric structure containing multiple ligands assembled by coordinative bonds. Experimental results have been complemented by modeling the electronic structure of isolated monomers and by building models for the polymeric structure.

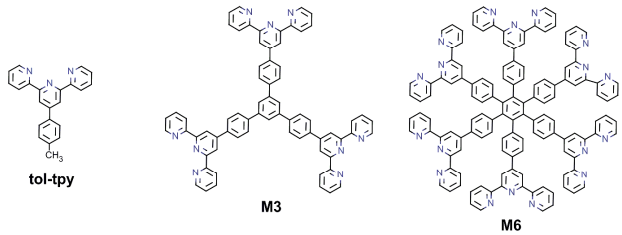

Scheme 1

Experimental section

M3 and **M6** were synthesized according to literature procedures.[11]

Photophysical measurements. The experiments were carried out in air-equilibrated dichloromethane solution at 298 K, unless otherwise noted. UV/Vis absorption spectra were recorded with a Perkin Elmer l40 spectrophotometer, using quartz cells with path length of 1.0 cm. Luminescence spectra were performed with a Perkin Elmer LS-50 or an Edinburgh FLS920 spectrofluorimeter, equipped with a Hamamatsu R928 phototube. Lifetimes were measured by the above mentioned Edinburgh FLS920 spectrofluorimeter equipped with a TCC900 card for data acquisition in time-correlated single-photon counting experiments (0.4 ns time resolution) with diode lasers. Emission quantum yields were measured following the method of Demas and Crosby[12] (standard used: quinine sulphate in H_2SO_4 0.5 M).[13] Estimated experimental errors are: 2 nm on the band maximum, 5% on molar absorption coefficients, emission intensities,

fluorescence lifetimes and log K values, 10% on fluorescence quantum yields.

Computational details. Atomic structures of **M6-45** and **M6-90** were optimized with density functional theory (DFT) calculations using the CAM-B3LYP hybrid functional with the 6-31G* basis set. Molecular orbital shapes and energies discussed in the text are calculated at the lowest energy optimized structures. Orbital and optimized geometry pictures were prepared with the Molekel visual software,[14] while structures of 3D and 2D polymers were prepared with pymol.[15] Electronic excitation energies and oscillation strengths were computed for the 30 lowest singlet excited electronic states of tol-tpy with time dependent (TD) DFT calculations employing both the B3LYP and CAM-B3LYP functionals. In plotting the computed electronic spectrum a Lorentzian line width of 0.3 eV was superimposed to all computed intensities to facilitate the comparison with the experimental spectrum. Computed spectra did not include vibronic structures associated with electronic bands. All quantum-chemical calculations were performed with the Gaussian09 package.[16]

Results and discussion

Photophysical properties of M3 and M6

For solubility reasons, all the photophysical data have been recorded in CH_2Cl_2 solution. The absorption spectra of **M3** and **M6** show a band with maximum at ca. 300 nm (Figure 1). Comparison with the absorption profile of 6 **tol-tpy** units (dashed green line in Figure 1, see also Figure S1 for a comparison between computed and observed **tol-tpy** spectra) shows that **M6** spectrum is not merely the sum of those of the model compounds. Similar considerations are valid in the case of **M3**. Also the emission spectra change going from **tol-tpy** to **M3** and **M6**, showing a progressive red shift of the maximum (Figure 1) and an increase in emission quantum yield: from 8% for **tol-tpy** to 37% and 34% for **M3** and **M6**, respectively. The corresponding excited state lifetimes (Table 1) are in the nanosecond time scale, as expected for a fluorescent excited state.

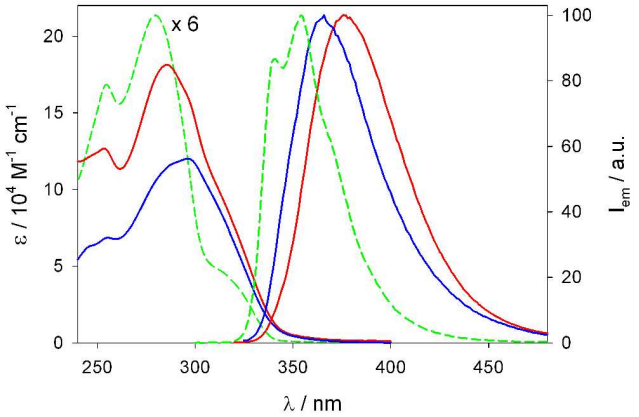

Figure 1. Absorption (left) and normalized emission spectra (right, upon excitation in the lowest energy band) of **M6** (red line), **M3** (blue line) and **tol-tpy** (green line) in CH_2Cl_2 solution at 298 K. For comparison purposes, the absorption spectrum of **tol-tpy** has been multiplied by 6.

Electronic interactions are responsible for the difference in the photophysical properties of the multi-terpyridine ligands compared to those of constituent units, i.e. **tol-tpy** and benzene, as it can be inferred from the computed frontier molecular orbitals of **M6** shown in Figure 2. The orbitals are delocalized because of electronic interactions. In addition, the orbital order has changed compared with that of the **tol-tpy** unit (see the orbitals depicted in the insets of Figure S1): the HOMO-1 of **tol-tpy** is related to the HOMO of **M6** shown in Figure 2. As a result, it can be expected that the lowest excited state of **M6** is related with the strongly absorbing state, thereby showing also an increased emission compared with **tol-tpy**.

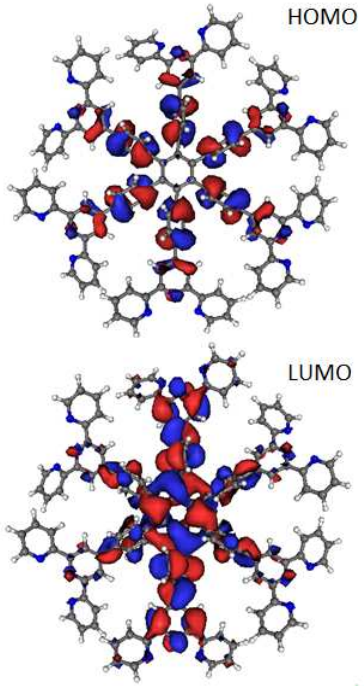

Figure 2. Delocalized character of the CAM-B3LYP/6-31G* computed molecular orbitals of **M6** at its optimized geometry.

Table 1. Photophysical data of **tpy**, **tol-tpy**, **M3** and **M6** in air-equilibrated CH_2Cl_2 solution at 298 K, unless otherwise noted.

	absorption		emission		
	λ_{max} / nm	ε_{max} / 10^4 M^{-1} cm^{-1}	λ_{max} / nm	Φ_{em}	τ / ns
tpy	280	1.6	336	0.003[a]	-
tol-tpy	280	3.6	340	0.08	1.7
M3	298	12.2	364	0.37	3.1
M6	286	18.2	376	0.34	1.6

aIn acetonitrile solution, from ref. 8.

M6 as ligand of Fe^{2+} ions: photophysical data

Titration of a 3.7×10^{-6} M solution of **M6** in CH_2Cl_2 with a 0.8 mM $Fe(CF_3SO_3)_2$ acetonitrile solution leads to (i) strong changes in the absorption spectra (Figure 3a) going from a colourless to a purple solution and (ii) to a complete quenching of the emission band at 376 nm (Figure 3b). From a qualitative point of view,

these spectral changes are similar to those obtained for the model compound **tol-tpy** (Figure 4): they are consistent with a charge perturbation effect of the ligand absorption band in the UV region and the appearance of a metal-to-ligand charge transfer (MLCT) band in the visible region, as expected for iron terpyridine based complexes.[17] Quenching of the fluorescence can be rationalized on the basis of the low-lying MLCT excited state of $[Fe(tpy)_2]^{2+}$ which is known to be non-luminescent because of a fast decay to the ground state via metal centered (MC) excited states.[18]

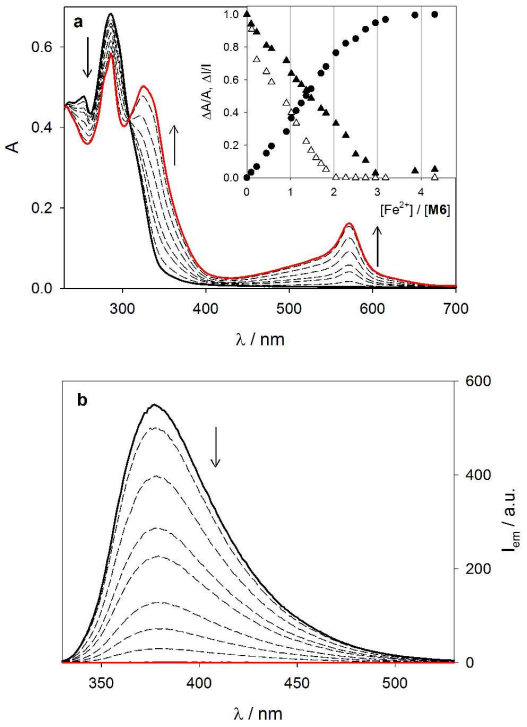

Figure 3. Absorption (a) and emission spectra (b) of a 3.7×10^{-6} M solution of **M6** in CH_2Cl_2 upon titration with $Fe(CF_3SO_3)_2$: 0 eq. (solid black line), 3.0 eq. (solid red line). λ_{ex} = 308 nm. Inset shows normalized absorption changes at 286 (solid triangles) and 326 nm (solid circles), and normalized emission changes at 377 nm (empty triangles).

From a quantitative point of view, in the case of **tol-tpy**, the plateau is reached at 0.5 eq. of Fe^{2+} per ligand, as clearly visible by the plot of the normalized absorption and emission intensity in the inset of Figure 4. This result is consistent with the formation of the $[Fe(\mathbf{tol\text{-}tpy})_2]^{2+}$ complex, as previously reported.[19] Job's plot is reported in Figure S4a. Global fitting analysis of the absorption changes by the SPECFIT software[20] leads to very high formation constant for $[Fe(\mathbf{tol\text{-}tpy})_2]^{2+}$ complex: log β_2 ca. 20. This value is too high to be precisely estimated by this technique, however it is very similar to that reported for tpy in water.[21]

For **M6**, normalized absorption spectral changes reach a plateau at 3 eq. of Fe^{2+} (Figure 3a, inset), i.e. at 0.5 eq. of Fe^{2+} per tpy unit, with no further change upon addition of up to 10 eqs. This result can be interpreted as follows: (i) as an average, roughly half of the tpy units of each **M6** molecule are engaged in formation of complexes with 1:1 stoichiometry, or (ii) complexes of $[Fe(tpy)_2]^{2+}$-type are formed, engaging all the tpy units present in each **M6** molecule. The first hypothesis is quite unlikely since all tpy units are readily accessible to metal ions and a 2:1 ligand to metal complex is formed with very high stability constant at low metal ion concentration in the case of the model compound **tol-tpy**. As to the second hypothesis, two tpy units of the same molecule cannot cooperate to bind a single metal ion since the ligand structure is quite rigid. Therefore, the most likely structure is a polymer in which each Fe^{2+} ion is complexed by two tpy units belonging to two different **M6** molecules (see pictorial representation in Scheme 2). Such issue has also been addressed through a rigid modeling of the Fe^{2+} complex with **M6**, as it is described below. Global fitting of the absorption spectra yields a very high stability constant for the 2:1 ligand to metal complex, not allowing an accurate estimation of its value by this technique.

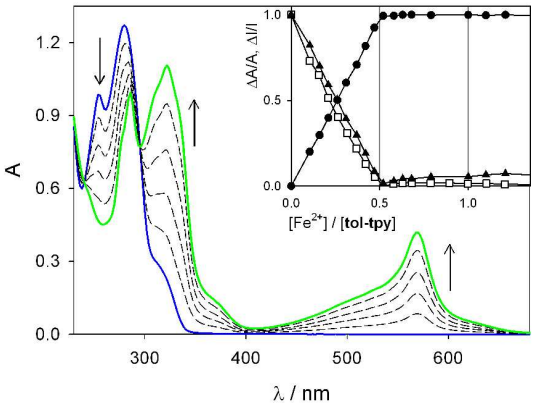

Figure 4. Absorption spectra of a 3.5×10^{-5} M solution of **tol-tpy** in CH_2Cl_2 upon titration with $Fe(CF_3SO_3)_2$: 0 eq. (solid blue line), 0.5 eq. (solid green line). Inset shows normalized absorption changes at 382 (solid triangles) and 570 nm (solid circles), and normalized emission changes at 388 nm (empty squares, λ_{ex} = 295 nm).

The emission intensity plot, obtained upon excitation at the isosbestic point at 308 nm, is not superimposed to that of the absorption decrease at 286 nm (Figure 3a, inset), at variance with the plots reported for the model **tol-tpy** ligand (Figure 4, inset). Upon addition of 1.5 eqs. of Fe^{2+} per **M6**, normalized absorption intensities are 50% of the value at the end of the titration, meaning that half of the tpy units are engaged in metal ion complexation, but the emission intensity of the free ligand is decreased to less than 20% of the initial value. This result points out the occurrence of interactions in the excited states between free and complexed tpy units of the same molecule as it is suggested by the delocalized nature of frontier molecular orbitals in Figure 2. Indeed, intermolecular interactions are ruled out by the ns-lifetime of the luminescent excited state and the low concentration of **M6** (micromolar range). The luminescent excited state of free **tol-tpy** units is quenched by either energy transfer to the complexed ones, characterized by low-energy excited states, or by electron transfer from $[Fe(tpy)_2]^{2+}$ units.

Modeling of Fe^{2+} metal complexes with M6

To investigate the likelihood of a polymeric structure where each Fe^{2+} ion is complexed by two tpy units, as well as to obtain more information about its spatial arrangement (either in a plane, as reported in Scheme 2 and observed at the air/water interface,[9] or a 3D arrangement), we modeled two different possible structures for **M6** oligomers.

The complexes were built starting from monomer, assumed in a given conformation, and linked to identical monomers (that is, featuring the same conformation) to every tpy moiety available. The modeling of polymeric structures was rigid – namely based on an addition of identical monomers rigidly translated and rotated.

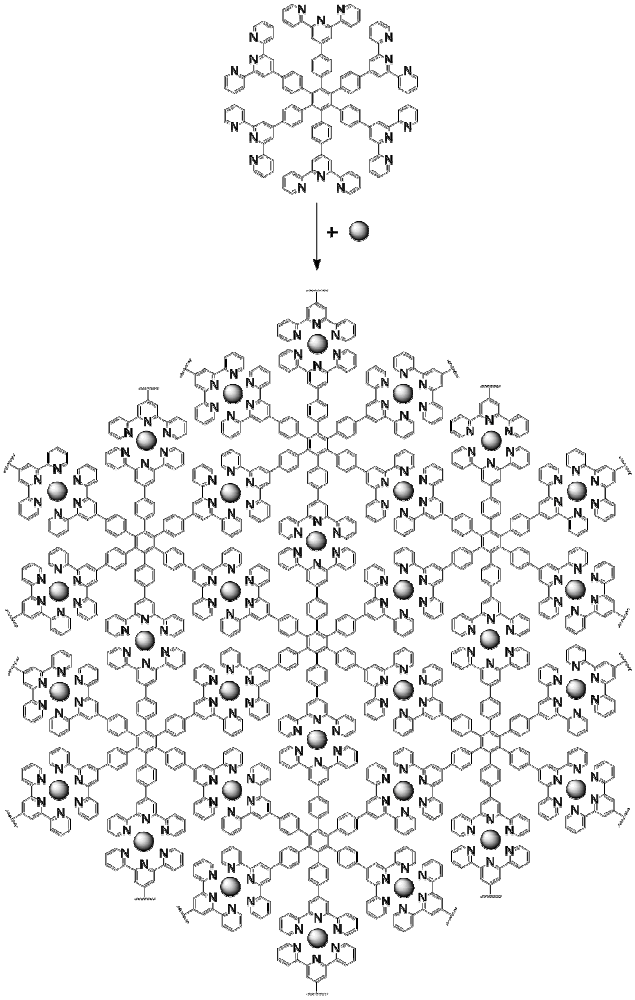

Scheme 2

Concerning the choice of the monomer conformation, we focused on two, a first featuring every tpy unit tilted of 45° with respect to the core plane (hereafter labeled **M6-45**) and a second with tpy units alternately orthogonal to or laying in the core plane (hereafter labeled **M6-90**), as shown in Figure 5.

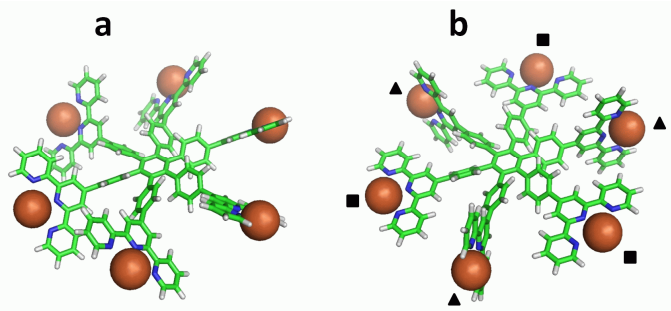

Figure 5. The two conformers of **M6** considered for building 2D or 3D polymeric structures: (a) **M6-45**, where every tpy unit is tilted of 45° with respect to the core plane and (b) **M6-90** monomers, where tpy units are alternately orthogonal (triangle) to or laying (square) in the core plane.

Geometry optimization of a single **M6** monomer at CAM-B3LYP/6-31G* level shows that conformer **M6-45** is 2.62 kcal/mol more stable than the optimized **M6-90** (Figure 6), where the originally perpendicular tpy units are considerably distorted. This suggests that the preferential unit for building polymeric structures is **M6-45** rather than **M6-90**.

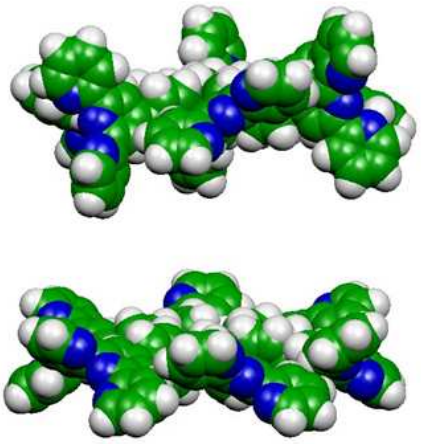

Figure 6. CAM-B3LYP/6-31G* optimized conformers of **M6**: (top) the less stable **M6-90** and (bottom) the more stable **M6-45** conformer.

Figure 7 shows the 2D polymer (a,c) and one possible 3D structure (b,d) built from **M6-45** conformers. For simplicity the 2D and 3D structures were built from non-optimized M6 units of Figure 5, but results would not change using optimized structures of Figure 6. Figure 7 (a,c) shows the second generation 2D oligomer, i.e. the central **M6** monomer (red) linked to two shells of M6 monomers (light yellow and green). It can be clearly seen how **M6-45** monomers lead to the already reported planar structure,[9] which could be obtained also from **M6-90** monomers, a possibility which is not further discussed, given their computed higher energy. The 3D structure in Figure 7 (b,d) is originated by a central M6-45 unit around which a defect is developed because of the alternate orientation and linking of the six M6 monomers (yellow in Figure 7) surrounding the central unit.

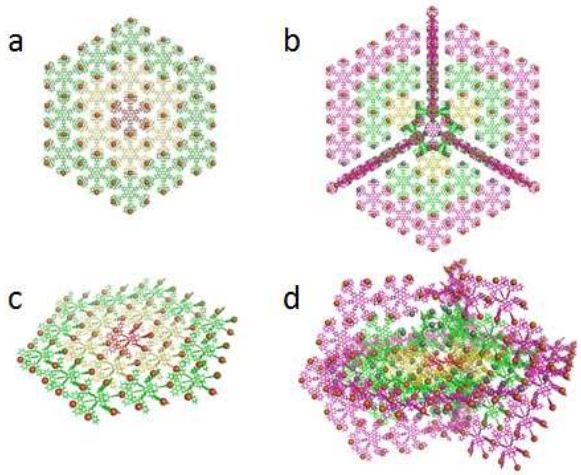

Figure 7. Models of 2D (a,c) and 3D (b,d) structures built using **M6-45** conformers. The core monomer is shown in red, the first generation row in yellow, the second generation row in green and the third generation (only for the 3D structure) in magenta; Fe^{2+} are shown as brown spheres when involved in 2:1 ligand to metal binding and grey for Fe^{2+} bound to only one tpy unit. See the discussion in the text.

This alternation triggers the development of three regions in which the typical 2D complexation develops, separated by three perpendicular planes, each rotated by 120 degrees around the central monomer C3 axis. The less stable **M6-90** conformer could also contribute to the development of 3D structures similar to that of Figure 7 (b,d) and shown Figure S2. A central (red in Figure S2) **M6-90** *defect* with the alternation of perpendicular and planar tpy units would also lead to a 3D structure. In both cases, we attribute the formation of a 3D structure to the presence of a *defect* since the development of the 3D structure is accompanied by an incomplete linking of metal ions to tpy units (see below). Note that the 3D structures in Figures 7 and S2 are only examples of the possible 3D structures that can be built from **M6** units. Others could be considered, for instance developing additional planes parallel to the main polymer plane in Figure 7b. More important, however, is the fact that in the 3D structures not all the *internal* tpy moieties can link to Fe^{2+} in a 2:1 ligand to metal ratio because of steric hindrance. This can be appreciated in Figure 7, where the metal ions linked to two tpy units are depicted in brown, while those linked to one tpy unit are grey. It is clear that the defect originating 3D structures is accompanied by a number of metal ions linked to only one tpy unit. On the other hand, for the planar network, all the *internal* tpy units are linked in a 2:1 ligand to metal ratio and the 1:1 ligand to metal ratio is limited to the peripheral tpy units. In view of the large stabilization associated with the formation of the 2:1 ligand to metal complexes, it can be concluded that a larger stability is expected for the 2D network. Moreover, because of the unfavorable ligand to metal ratio, a structure containing a number of defects triggering the 3D structure is not consistent with the photophysical results showing a plateau at 0.5 eqs. of Fe^{2+} per tpy unit. The total number of Fe^{2+} ions linked to tpy units in the 2D and the proposed 3D structure (either in a 1:1 or in a 2:1 ligand to metal ratio) has been calculated for increasingly larger 2D and 3D networks and is reported in Table 2 along with the total number of available tpy units.

Table 2. Total number of metal ions linked and total number of tpy units available for increasingly larger generations of 2D and 3D networks of **M6** and their ratio. The ratio decreases from 1 and tends to 0.5 for increasingly large 2D networks.

Oligomer generation	No. Fe^{2+} ions	No. tpy units	No. Fe^{2+} / No. tpy
	2D structure		
Monomer	6	6	1.00
1	30	42	0.714
2	72	114	0.632
3	132	222	0.595
4	210	366	0.574
5	306	546	0.560
6	420	762	0.551
7	552	1014	0.544
8	702	1302	0.539
	3D structure		
Monomer	6	6	1.00
1	36	42	0.857
2	144	186	0.774
3	288	414	0.696
4	486	738	0.659
5	714	1134	0.630

The ratio between the two numbers decreases with the increase of the 2D network and tends to 0.5 in very good agreement with the experimental results discussed above. The ratio also decreases with increasing the dimension of the 3D structure but more slowly. In addition it should be noted that the 3D structure in Figure 7 contains only a single defect, while a larger number of defects driving more rigid 3D structure would slow further down the ratio decrease. Based on the data of Table 2, it can also be concluded that the dimension of the 2D networks generated by complexation is expected to be relatively large to account for the observed value of the eq. of Fe^{2+} per ligand, since small oligomeric structures would lead to considerably larger values (0.7 and 0.6 for generations 1 and 3, respectively) of eq. of Fe^{2+} per tpy.

M6 as ligand of Zn^{2+} ions

Titration of a 5.3×10^{-6} M solution of **M6** in CH_2Cl_2 with a 1.8 mM $Zn(CF_3SO_3)_2$ solution causes the decrease of the absorption band at 286 nm and the increase of a new band at 340 nm (Figure 8a), with isosbestic points at 316 nm between 0 and 1.2 eqs. of Zn^{2+} and at 312 nm from 1.2 to the end of the titration. Similar spectral changes have been observed for **tol-tpy** upon titration with Zn^{2+} ions and they are consistent with a charge perturbation effect on the ligand centered absorption and emission bands, as previously reported in the literature.[8,22,23,24]

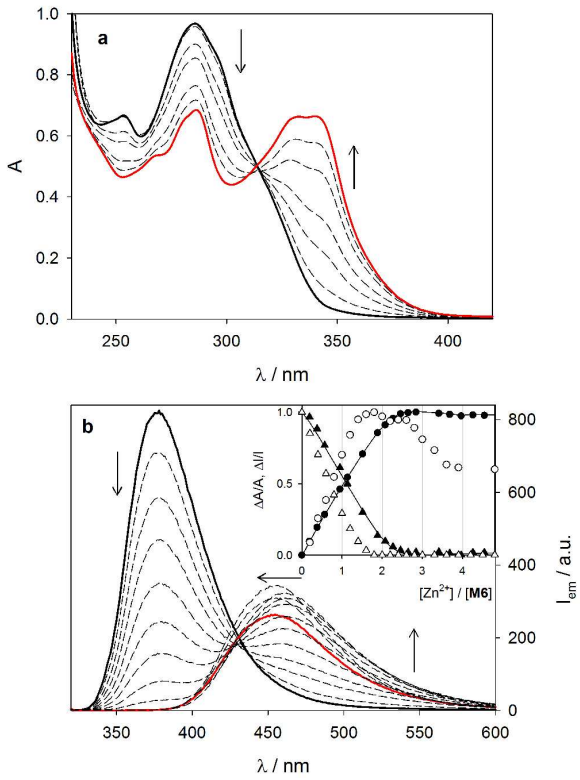

Figure 8. Absorption (a) and emission spectra (b) of a 5.3 × 10^{-6} M solution of **M6** in CH_2Cl_2 upon titration with $Zn(CF_3SO_3)_2$: 0 eq. (solid black line), 3.0 eqs. (solid red line). λ_{ex} = 315 nm. Inset shows normalized absorption changes at 285 (solid triangles) and 343 nm (solid circles), and normalized emission changes at 378 (empty triangles) and 500 nm (empty circles); solid lines represents the fitting by SPECFIT (for more details, see text).

For **tol-tpy**, spectral changes demonstrate the formation of $[Zn(\mathbf{tol\text{-}tpy})_2]^{2+}$ complex at low metal ion concentration, replaced by $[Zn(\mathbf{tol\text{-}tpy})]^{2+}$ complex upon further addition of metal ions (Figure S3). Global fitting of the absorption spectra yields very high formation constants for the 1:1 (β_1) and 1:2 (β_2) metal to ligand stoichiometry: log β_1 = 8.2, log β_2 = 15.7.

In the case of **M6**, normalized absorption changes reach a plateau at ca. 3 eqs. of metal ion per **M6** molecule with no further change upon addition of up to 10 equivalents (Figure 8b, inset). On the basis of the previous discussion, this result can be interpreted by formation of the polymeric structure reported in Scheme 2. Global fitting of the absorption spectra reaches a good match with experimental data by taking into account formation of complexes of 1:1, 2:1, and 3:1 ligand (**M6**) to metal stoichiometry: log β_1 = 6.2, log β_2 = 13.3 log β_3 = 19.0. In agreement with the data reported in the literature,[1] the binding constant of tpy ligands for Zn^{2+} are lower than those for Fe^{2+}.

Upon excitation at 316 nm, a decrease of the emission band at 376 nm is accompanied by the appearance of a lower energy band which increases up to 1.8 eqs. and then shifts toward the blue while slightly decreasing in intensity (Figure 8b). Absorption and emission intensity changes as a function of the metal ion concentration are clearly different from each other (Figure 8b, inset). Before reaching the plateau, emission plots are much steeper than absorption ones. On the contrary, the first part of the titration of **tol-tpy** with Zn^{2+} shows overlapped absorption and emission changes (Figure S3). In the case of **M6**, at 1.1 eqs. of Zn^{2+}, the normalized absorbance variation accounts for 50% of the total absorption changes, while the emission intensity at 378 and 500 nm reach 80% of the maximum variation. The corresponding excitation spectrum, recorded at λ_{em} = 500 nm, shows a close match with the corresponding absorption spectrum. This indicates an efficient energy transfer between free and complexed moieties of the same molecule which explains the faster variations underwent by the emission intensity profiles. Intermolecular interaction can be ruled out as previously discussed. Upon further addition of metal ion, in particular between 2 and 3.5 eqs. of Zn^{2+} per molecule, the spectral variations undergone by the low energy emission band are likely due to a charge perturbation effect, consistent with the increase of the number of Zn^{2+} ions per molecule. Upon addition of 3 eqs. of Zn^{2+} (red line in Figure 8b) a species with Φ_{em} = 14% is obtained.

Fe^{2+} and Zn^{2+} metal complexes with M3

In the case of **M3**, titration of a 3.6 × 10^{-6} M solution in CH_2Cl_2 with $Fe(CF_3SO_3)_2$ leads to analogous absorption and emission spectral changes with respect to those observed for **M6**, and the plateau is reached at 1.5 eq. of Fe^{2+} per **M3** molecule, i.e. at 0.5 eq. of metal ion per tpy unit. Also in this case the results suggest the formation of the same structure in which each Fe^{2+} ion is coordinated by two tpy units of two different **M3** molecules.

Upon titration of the same solution with $Zn(CF_3SO_3)_2$, absorption spectral changes similar to those reported in Figure 8a have been reported with a plateau at 1.5 eqs. of metal ions. The emission spectra (Figure 9) performed upon excitation at 321 nm (isosbestic point) show a decrease of the band at 364 nm, and the appearance of a new band at 412 nm which reaches its maximum at 0.5 eq. and then decreases in intensity and shifts toward the red reaching a plateau at 1.5 eqs. with λ_{max}= 465 nm. These results suggest the formation of complexes with different ratios of metal ions to **M3**.

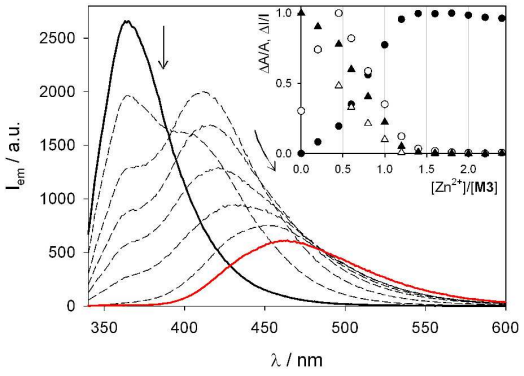

Figure 9. Emission spectra of a 3.6 × 10^{-6} M solution of **M3** in CH_2Cl_2 upon titration with $Zn(CF_3SO_3)_2$: 0 eq. (solid black line), 1.5 eqs. (solid red line). λ_{ex} = 315 nm. Inset shows normalized absorption changes at 298 (solid triangles) and 343 nm (solid circles), and normalized emission changes at 364 (empty triangles) and 412 nm (empty circles).

Conclusions

The investigated multi-terpyridine ligands **M3** and **M6** display

high luminescence in the spectral region between near UV and blue, compared to the very weak luminescence of pristine terpyridine. Based on preliminary quantum-chemical investigations on **tol-tpy** and **M6**, it is suggested that the different emission properties are due to a different orbital nature of the emitting excited state. Metal complexation brings about strong changes in the photophysical properties: the Fe^{2+} complex is purple and not-emissive, while the Zn^{2+} complex is colourless and blue emitting. The most interesting result is the formation of a polymeric structure upon metal ion complexation. In the case of Fe^{2+} and **M6**, each metal ion is bound to two tpy units of two different ligands, as suggested by the fact that absorption spectral changes reach a plateau at 3 eqs. of metal ions per **M6**, i.e. at 0.5 eq. of metal ion per tpy unit. By modeling realistic 2D and 3D structures, we concluded that, in analogy to previous findings at the air/water interface, a dominant 2D network is formed in solution. It is likely that, differently from the air/water interface, in solution the structure is partially folded. Our results show that, although the presence of 3D defects cannot be ruled out, their concentration should be definitely small to account for the observed ligand to metal ratio.

These findings disclose important information for the construction of 2D metal coordination polymers, a new and challenging research field that is intended to propose new candidates for molecular sieves, ultrasensitive pressure-sensors, and surface coatings.

Acknowledgments

We thank Dr. Thomas Bauer for providing the compounds. We gratefully acknowledge MIUR (FIRB RBAP11C58Y, PRIN 2010N3T9M4) for financial support.

Notes and references

[a] *Department of Chemistry "G. Ciamician", University of Bologna, Via Selmi 2, 40126 Bologna, Italy, e-mail: paola.ceroni@unibo.it*
[b] *Department of Materials, ETH Zürich, HCI J 541, CH-8093 Zürich, Switzerland*

† Electronic Supplementary Information (ESI) available: Photophysical and modeling data. See DOI: 10.1039/b000000x/

1 U. S. Schubert, H. Hofmeier and G. R. Newkome, Modern Terpyridine Chemistry, Wiley-VCH, Weinheim, Germany, 2006.

2 (a) A. Wild, A. Winter, F. Schlütter and U. S. Schubert, Advances in the field of π-conjugated 2,2′:6′,2″-terpyridines, *Chem. Soc. Rev*., 2011, **40**, 1459. (b) E. C. Constable, 2,2′:6′,2″-Terpyridines: From chemical obscurity to common supramolecular motifs, *Chem. Soc. Rev*., 2007, **36**, 246

3 (a) C. W. Machan, M. Adelhart, A. A. Sarjeant, C. L. Stern, J. Sutter, K. Meyer and C. A. Mirkin, One-Pot Synthesis of an Fe(II) Bis-Terpyridine Complex with Allosterically Regulated Electronic Properties, *J. Am. Chem. Soc.* 2012, **134**, 16921. (b) F. Barigelletti and L. Flamigni, Photoactive molecular wires based on metalcomplexes, *Chem. Soc. Rev*., 2000, **29**, 1.

4 C. R. K. Glasson, L. F. Lindoy and G. V. Meehan, Recent developments in the d-block metallo-supramolecular chemistry of polypyridyls, *Coord. Chem. Rev*., 2008, **252**, 940. (b) F. Puntoriero, S. Campagna, A. M. Stadler and J.-M. Lehn, Luminescence properties and redox behavior of Ru(II) molecular racks, *Coord. Chem. Rev*., 2008, **252**,2480.

5 For some recent examples, see: (a) X. Lu, X. Li, Y. Cao, A. Schultz, J.-L. Wang, C. N. Moorefield,C. Wesdemiotis, S. Z. D. Cheng and G. R. Newkome, Self-Assembly of a Supramolecular, Three-Dimensional, Spoked, Bicycle-like Wheel, *Angew. Chem. Int. Ed.,* 2013, **52**,7728. (b) A. Schultz, X. Li, B. Barkakaty, C. N. Moorfield, C. Wesdemiotis, G. R. Newkome, Stoichiometric Self-Assembly of Isomeric, Shape-Persistent, Supramacromolecular Bowtie and Butterfly Structures, *J. Am. Chem. Soc.*, 2012, **134**, 7672. (c)Y.-T. Chan, X. Li, J. Yu, G. A. Carri, C. N. Moorefield, G. R. Newkome and C. Wesdemiotis, Design, Synthesis, and Traveling Wave Ion Mobility Mass Spectrometry Characterization of Iron(II)– and Ruthenium(II)–Terpyridine Metallomacrocycles, *J. Am. Chem. Soc.*, 2011, **133**, 11967. (d) J.-L. Wang, X. Li, X. Lu, I.-F. Hsieh, Y. Cao, C. N. Moorefield, C. Wesdemiotis, S. Z. D. Cheng and G. R. Newkome, Stoichiometric Self-Assembly of Shape-Persistent 2D Complexes: A Facile Route to a Symmetric Supramacromolecular Spoked Wheel, *J. Am. Chem. Soc*., 2011, **133**, 11450.

6 (a) P. R. Andres and U. S. Schubert, New Functional Polymers and Materials Based on 2,2′:6′,2″-Terpyridine Metal Complexes, *Adv. Mater*., 2004, **16**, 1043. (b) U. S. Schubert and C. Eschbaumer, Macromolecules Containing Bipyridine and Terpyridine Metal Complexes: Towards Metallosupramolecular Polymers, *Angew. Chem. Int. Ed.*, 2002, **41**, 2892.

7 For some recent examples, see e.g.: (a) J. Zhan, Q. Hu, Q. Wu, C. Li, H. Qiu, M. Zhang and S. Yin, A stimuli-responsive orthogonal supramolecular polymer network formed by metal–ligand and host–guest interactions, *Chem. Commun*., 2014, **50**, 722. (b) J. K. Molloy, P. Ceroni, M. Venturi, T. Bauer, J. Sakamoto and G. Bergamini, Self-assembly of nanocrystalline tetra-terpyridine complexes: from molecules to mesoscopic objects, *Soft Matter*, 2013, **9**, 10754. (c) K. Zhang, Y. Zha, B. Peng, Y. Chen and G. N. Tew, Metallo-Supramolecular Cyclic Polymers, *J. Am. Chem. Soc*. 2013, **135**, 15994. (d) T. Bauer, Z. Zheng, A. Renn, R. Enning, A. Stemmer, J. Sakamoto and A. D. Schlüter, Synthesis of Free-Standing, Monolayered Organometallic Sheets at the Air/Water Interface, *Angew. Chem. Int. Ed.*, 2011, **50**, 7879. (e) I. Eryazici, O. K. Farha, O. C. Compton, C. Stern, J. T. Hupp and S. T. Nguyen, Luminescent infinite coordination polymer materials from metal-terpyridine ligation *Dalton Trans*. 2011, **40**, 9189.

8 G. Albano, V. Balzani, E.C. Constable, M. Maestri, and D.R. Smith, Photoinduced processes in 4'-(9-anthryl)-2,2' :6',2"-terpyridine its protonated forms and Zn (II), Ru (II) and Os (II) complexes, *Inorg. Chim. Acta*. 1998, **277**, 225.

9 T. Bauer, Z. Zheng, A. Renn, R. Enning, A. Stemmer, J. Sakamoto and A. D. Schlüter, Synthesis of Free-Standing, Monolayered Organometallic Sheets at the Air/Water Interface, *Angew. Chem. Int. Ed.* 2011, **50**, 7879.

10 Z. Zheng, C. S. Ruiz-Vargas, T. Bauer, A. Rossi, P. Payamyar, A. Schütz, A. Stemmer, J. Sakamoto and A. D. Schlüter, Square-Micrometer-Sized, Free-Standing Organometallic Sheets and Their Square-Centimeter-Sized Multilayers on Solid Substrates, *Macromol. Rapid Commun.* 2013, **34**, 1670.

11 T. Bauer, A. D. Schlüter and J. Sakamoto, Towards 2D and 3D Coordination Polymers: Synthesis of Shape-Persistent Star Monomers with 2,2′:6′,2″-Terpyridin-4′-yl Units at the Periphery, *Synlett.* 2010, 877

12 J. N. Demas and G. A. Crosby, Measurement of photoluminescence quantum yields. Review, *J. Phys. Chem.* 1971, **75**, 991.

13 A. M. Brouwer, Standards for photoluminescence quantum yield measurements in solution, *Pure Appl. Chem*. 2011, **83**, 2213.
14 Molekel, version 4.3 and 5.4, http://www.cscs.ch/molekel/; Portmann, S.; Lüthi, H. P. Chimia 2000, 54, 766.
15 PYMOL0.99 (http://pymol.sourceforge.net/).
16 M. J. Frisch et al. Gaussian 09, revision A.02; Gaussian, Inc., Wallingford CT, 2009.
17 P. S. Braterman, J.-I. Song and R. D. Peacock, Electronic absorption spectra of the iron(II) complexes of 2,2'-bipyridine, 2,2'-bipyrimidine, 1,10-phenanthroline, and 2,2':6',2''-terpyridine and their reduction products, *Inorg. Chem.* 1992, **31**, 555 and references therein.
18 C. Creutz, M. Chou, T. L. Netzel, M. Okumura and N. Sutin, Lifetimes, spectra, and quenching of the excited states of polypyridine complexes of iron(II), ruthenium(II), and osmium(II), *J. Am. Chem. Soc.* 1980, **102**, 1309.
19 E. Amouyal and M. Mouallem-Bahout, Photophysical study of tolylterpyridine complexes. Intramolecular electron transfer in an osmium(II) dyad, *J. Chem. Soc. Dalton Trans.* 1992, 509.
20 (a) R. A. Binstead, SPECFIT; Spectrum Software Associates: Chapell Hill, NC, 1996. (b) H. Gampp, M. Maeder, C. J. Meyer and A. Zuberbulher, Calculation of equilibrium constants from multiwavelength spectroscopic data—II[1]**32**, 95.: Specfit: two user-friendly programs in basic and standard fortran 77, *Talanta* 1985, **32**, 257.
21 U. S. Schubert, H. Hofmeier and G. R. Newkome, *Modern Terpyridine Chemistry*, Wiley-VCH,Weinheim, 2006, ch. 4.
22 X. Chen, Q. Zhou, Y. Cheng, Y. Geng, D. Ma, Z. Xie and L. Wang, Synthesis, structure and luminescence properties of zinc (II) complexes with terpyridine derivatives as ligands, *J. Lumin.* 2007, **126**, 81.
23 L. J. Liang, X. J. Zhao and C. Z. Huang, Zn(II) complex of terpyridine for the highly selective fluorescent recognition of pyrophosphate, *Analyst* 2012, **137**, 953.
24 M. Presselt, B. Dietzek, M. Schmitt, J. Popp, A. Winter, M. Chiper, C. Friebe and U. S. Schubert, Zinc(II) Bisterpyridine Complexes: The Influence of the Cation on the π-Conjugation between Terpyridine and the Lateral Phenyl Substituent, *J. Phys. Chem. C* 2008, **112**, 18651.

Table of content

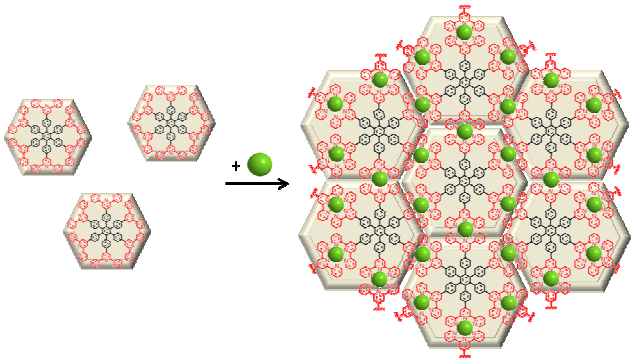

Metal ion coordination by a hexaterpyridince ligand induces the formation of a 2D network in dichloromethane solution as demonstrated by photophysical and modeling studies.